

AperTO - Archivio Istituzionale Open Access dell'Università di Torino

Solid lipid nanoparticles produced through a coacervation method

This is the author's manuscript

Original Citation:

Availability:

This version is available <http://hdl.handle.net/2318/61349> since

Published version:

DOI:10.1080/02652040903031279

Terms of use:

Open Access

Anyone can freely access the full text of works made available as "Open Access". Works made available under a Creative Commons license can be used according to the terms and conditions of said license. Use of all other works requires consent of the right holder (author or publisher) if not exempted from copyright protection by the applicable law.

(Article begins on next page)



UNIVERSITÀ DEGLI STUDI DI TORINO

This is an author version of the contribution published on:

Questa è la versione dell'autore dell'opera:

Journal of Microencapsulation, vol. 27, Issue 1, 2010, p. 48-85

DOI 10.3109/02652040903031279

The definitive version is available at:

La versione definitiva è disponibile alla URL:

<http://informahealthcare.com/doi/full/10.3109/02652040903031279>

Solid lipid nanoparticles produced through a coacervation method

Luigi Battaglia, Marina Gallarate, Roberta Cavalli, Michele Trotta

Abstract: Solid lipid nanoparticles (SLN) of fatty acids (FAs) were prepared with a new, solvent-free technique based on FAs precipitation from their sodium salt micelles in the presence of polymeric non-ionic surfactants: this technique was called 'coacervation'. Myristic, palmitic, stearic, arachidic and behenic acid were employed as lipid matrixes. Spherical shaped nanoparticles with mean diameters ranging from 250 to ~500 nm were obtained. Different aqueous acidifying solutions were used to precipitate various FAs from their sodium salt micellar solution. Good encapsulation efficiency of Nile Red, a lipophilic model dye, in stearic acid nanoparticles was obtained. The coacervation method seems to be a potentially suitable technique to prepare close to monodisperse nanoparticles for drug delivery purposes.

Introduction

Solid lipid nanoparticles (SLN) are disperse systems with mean diameters ranging between 50–1000 nm and represent an alternative to polymeric particulate carriers. The main advantage of lipid carriers in drug delivery is the use of physiological lipids or lipid molecules with a history of safe use in therapy (Müller et al. 2000). Several SLN production methods are described in the literature: cold and hot homogenization (Müller and Lucks 1996), microemulsion dilution (Gasco 1993), microemulsion cooling (Mumper and Jay 2006), solvent evaporation (Siekmann and Westesen 1996) and solvent injection (Schubert and Müller-Goymann 2003). Recently, the authors developed an emulsification-diffusion technique using solvents with low toxicity, such as butyl lactate (Gallarate et al. 2008), isobutyric (Trotta et al. 2005) and isovaleric acid (Battaglia et al. 2007).

All the mentioned methods, except cold homogenization, allow one to obtain small nanoparticles, but each of them presents some disadvantages, such as the need of complex machines in high pressure homogenization, the toxicity of most solvents employed in solvent-based methods and the requirement of high temperatures to melt the lipid matrix in solvent-free methods. Moreover, the need to overcome patented methods leads to the development of potential alternative techniques for SLN production.

The aim of this work was the development of a new, solvent-free technique to produce SLN of fatty acids by acidification of a micellar solution of their alkaline salts. As pH is lowered, fatty acids precipitate owing to proton exchange between the acid solution and the soap: this process can be defined as 'coacervation'. The use of coacervation to produce polymeric nanoparticles is widely reported in the literature (Silva et al. 2008, Maculotti et al. 2008), but so far this technique has never been used for lipid nanoparticles production.

In this work, primary conditions to produce SLN for pharmaceutical applications were investigated by using myristic, palmitic, stearic, arachidic and behenic acid as lipid matrices and various molecular weight (Mw) partially hydrolysed polyvinyl alcohols and hydroxypropylmethyl cellulose as stabilizers. The stabilizers were chosen among non-ionic polymeric surfactants, since the absence of ionic groups makes them slightly sensitive to ionic strength and pH shifts. Nile Red, a lipophilic model dye, was chosen to study encapsulation efficiency within SLN.

Materials and methods

Materials

Citric acid, phosphoric acid, lactic acid, disodium hydrogenphosphate and sodium dihydrogenphosphate were from A.C.E.F. (Fiorenzuola d'Arda, Italy), 98% hydrolysed PVA 14 000–21 000 Mw (PVA 14 000) was from BDH Chemicals (Poole, UK); 80% hydrolysed PVA 9000–10 000 Mw (PVA 9000), 89% hydrolysed PVA 85 000–124 000 Mw (PVA 85 000),

sodium myristate (Na-M) and trehalose were from Sigma (Dorset, UK); sodium stearate (Na-S), sodium palmitate (Na-P), myristic acid (MA), palmitic acid (PA), arachidic acid (AA), behenic acid (BA) and Nile Red were from Fluka (Buchs, Switzerland); HPMC 2910 (hydroxypropylmethyl cellulose, 28–30% methyl substitution degree, 7–12% isopropyl substitution degree) 15cP (Benecel® E15—14 000 Mw), 50cP (Benecel® E50—21 000 Mw) and 4000cP (Benecel® E4M—86 000 Mw) were from Eigenmann & Veronelli (Rho, Italy); stearic acid (SA) was from Merck (Darmstadt, Germany). Sodium arachidate (Na-A) and sodium behenate (Na-B) were obtained by adding a stoichiometric amount of NaOH ethanolic solution to the ethanolic solution of arachidic and behenic acid: the soaps were purified by recrystallization and stored in an essicator at room temperature. Deionized water was obtained by a MilliQ® system (Millipore, Bedford, MO). All other chemicals were analytical grade and used without any further purification.

Methods

Determination of FA sodium salts Krafft point

Krafft point is defined as the temperature at which the solubility increases drastically with temperature (Shinoda 1967). Krafft point can normally be estimated by measuring the temperature above which surfactant and water dispersions transform to a clear solution over a wide concentration range (Wen and Franses 2000). Phase behaviour studies of different sodium soaps in aqueous solution were carried out by visual observation of the phases present in mixtures of known composition as a function of temperature (Lin et al. 2005), 1 w/w% soap aqueous solutions were sealed in closed test tubes with lids and Teflon tapes. The samples were submerged in a thermostatic water bath and equilibrated at various temperatures using a magnetic stirrer. Samples were first heated to 85°C and then slowly cooled to room temperature, leading to the precipitation of soap crystals. The Krafft point of sodium soap, which is the temperature at which the last crystal dissolves and the solution becomes isotropic and transparent, was then determined by heating each sample at 0.5°C min⁻¹.

PVA and HPMC viscosity determination

Viscosities of 1% w/w aqueous solutions of PVA and HPMC were determined at 50.0 ± 0.5°C in the presence of 1.07% w/w Na-S (corresponding to 1% w/w SA) by using an AVS 300 capillary viscometer (Schott Geräte, Germany).

SLN preparation

Different operative conditions were used for SLN preparation according to the FA under study. Stock solutions of each polymeric stabilizer were prepared by heating the polymer in water (PVA 9000: 25°C; PVA 14 000: 80°C; PVA 85 000: 80°C; HPMC: 25°C) and then cooling at room temperature. Each FA sodium salt was dispersed in the polymeric stabilizer stock solution and the mixture was then heated under stirring (300 rpm) just above the Krafft point of FA sodium salt to obtain a clear solution. A selected acidifying solution (coacervating solution) was then added drop-wise until pH ~ 4.0 was reached. The obtained suspension was then cooled in a water bath under stirring at 300 rpm until 15°C temperature was reached.

SLN characterization

SLN were characterized by TEM (CM 10 Philips, The Netherlands) spraying the SLN suspension on the microscope grid by means of an aerosol-sampling device.

Particle size and polydispersity of SLN dispersions were determined by the laser light scattering technique—LLS (Brookhaven, USA). Measurements were obtained at 90° angle on the appropriate water-diluted samples.

Thermograms were performed with a DSC 7 (Perkin-Elmer, USA). Lipid bulk material and SLN suspensions were placed in conventional aluminium pans and heated from 30° to 90°C at 2°C min⁻¹. The degree of crystallinity of SLN was estimated by calculating the ratio between the melting enthalpy/g lipid in SLN dispersion and the melting enthalpy/g of the bulk material (Siekman and Westesen 1994, Freitas and Müller 1999).

X-rays analysis was performed as follows: SLN suspension was centrifuged at 25 000 rpm for 30 min (Beckman Allegra® 64R Ultracentrifuge, USA) and washed twice with water, the precipitate was dried in vacuum overnight and analysed through a Guinier Camera 670 (Huber Diffraktionstechnik GmbH & Co., Germany).

SLN freeze-drying

SLN suspensions were freeze-dried without adding any cryoprotectant (FD-SLN) and in the presence of 5% w/v threosulose (FD-THR-SLN) by using a Modulyo Freeze Dryer (Edwards Alto Vuoto, Italy). Freeze-dried samples were then redispersed in water and analysed for size determination.

Nile Red-loaded SLN preparation

Nile Red-loaded 1% w/w SA-SLN were prepared by dissolving the dye in a minimum amount of ethanol, in order to enhance the rate of inclusion within micelles, and then adding this solution to the warm (50°C) aqueous Na-S solution. Lipid coacervation was then performed as previously described. The dye concentration was 6 $\mu\text{g mL}^{-1}$ in the soap solution. Encapsulation efficiency was calculated as the ratio between Nile Red amount in SLN and that in the starting micellar solution. Nile Red analysis was performed as follows: 1 ml SLN suspension was centrifuged, the supernatant was discharged, the precipitate was dried under vacuum overnight and then dissolved in 1 ml ethanol, which was injected in HPLC for Nile Red quantification. HPLC analysis was performed using a LC9 pump (Shimadzu, Japan) with an Allsphere ODS-2 5 μm 150 \times 4.6 mm column and a C-R5A integrator (Shimadzu, Japan); mobile phase: CH₃CN/H₂O 90/10 (flow rate = 1 mL min⁻¹); detector: RF551 Fluorimeter (Shimadzu, Japan) λ_{exc} = 546 nm; λ_{em} = 630 nm. The retention time was 4.5 min. SLN were also observed with a DM2500 fluorescence microscope (FM) (Leica, Germany).

Results and discussion

As preliminary screening, several 1% SLN dispersions were produced in the presence of PVA 9000, in order to individuate the appropriate coacervating solution to obtain homogeneously dispersed nanoparticles. The experimental conditions are reported in Table 1. As it can be noted, different coacervating solutions were required for the different fatty acids and increasing amounts of PVA 9000 were necessary to stabilize the suspensions of increasing chain length FA-SLN. Real difficulties are found to explain the empirically obtained operative conditions on the basis of physical and chemical considerations. Anyway, some general considerations on the coacervation process can be done. First of all, to obtain spherical nanoparticles, a pH of ~ 4.0 has to be reached before cooling, otherwise needle-like crystals will be formed. Next, the presence of a polymer is essential to avoid particle aggregation, probably because it acts like a steric stabilizer (Scholes et al. 1999).

	MA-SLN	PA-SLN	SA-SLN	AA-SLN	BA-SLN
Na-M	219 mg				
Na-P		217 mg			
Na-S			215 mg		
Na-A				214 mg	
Na-B					212 mg
PVA 9000	100 mg	200 mg	200 mg	4.00 mg	4.00 mg
Water	to 20 ml	to 20 ml	to 20 ml	to 20 ml	to 20 ml
1M Na ₂ HPO ₄	0.2 ml*				
1M citric ac.	1 ml*	0.4 ml			
1M lactic ac.			1 ml		
1M NaH ₂ PO ₄				0.4 ml**	0.4 ml***
1M H ₃ PO ₄				0.6 ml**	
1M HCl					0.6 ml***
Krafft point	4.0.5 ± 0.5°C	4.9.8 ± 0.5°C	4.7.2 ± 0.5°C	69.8 ± 0.5°C	74.3 ± 0.5°C

*mixed together and then added to Na-M micellar solution; **added to Na-A micellar solution as follows: NaH₂PO₄ and then H₃PO₄; ***added to Na-B micellar solution as follows: NaH₂PO₄ and then HCl.

Table 1. Experimental conditions for 1% w/v FA-SLN aqueous dispersions

TEM micrographs of FA-SLN showed particles spherical in shape and with regular and smooth surfaces: as an example the micrograph of SA-SLN obtained in the presence of PVA 9000 is reported in Figure 1. Mean diameters and polydispersity of SLN, determined by LLS, are reported in Table 2 and are comprised in the 250–500 nm range: MA-SLN presented the highest mean sizes and polydispersity. The differences in mean sizes among FA-SLN prepared can probably be related to a number of factors, such as operating temperature, FA chain length and PVA 9000 concentration, which varied in the production process of the different FA-SLN.

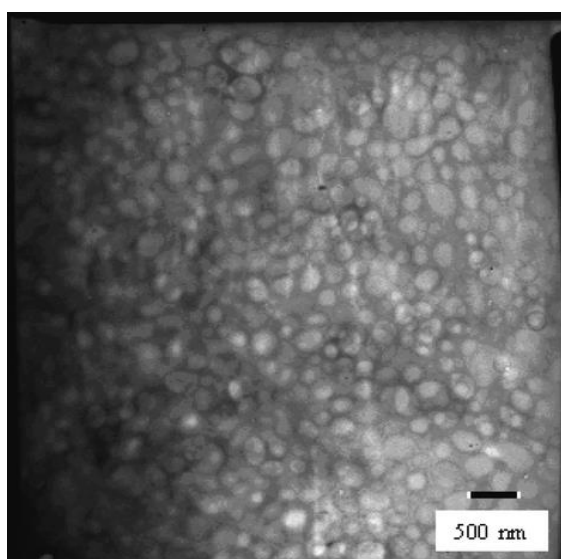


Figure 1. TEM micrograph of 1% SA-SLN.

	SLN		FD-SLN		FD-THR-SLN	
	Mean size (nm)	Polydispersity	Mean size (nm)	Polydispersity	Mean size (nm)	Polydispersity
MA-SLN	528 ± 55	0.207	—	—		
PA-SLN	263 ± 12	0.018	267 ± 14	0.076	269 ± 11	0.050
SA-SLN	285 ± 11	0.015	315 ± 15	0.170	300 ± 14	0.101
AA-SLN	315 ± 17	0.023	370 ± 20	0.076	358 ± 18	0.084
BA-SLN	373 ± 22	0.112	552 ± 60	0.249	375 ± 20	0.086

Table 2 Mean sizes and polydispersities of 1% w/v FA SLN before and after freeze-drying.

To verify the possibility to obtain a solid formulation, 1% w/v FA-SLN suspensions were freeze-dried in the absence of cryoprotectants (FD-SLN) and in the presence of 5% w/v threalose (FD-THR-SLN). SLN mean diameters and polydispersities before and after freeze-drying are reported in Table 2. Similar values in mean diameters were obtained for PA-SLN, SA-SLN and AA-SLN freeze-dried without any cryoprotectant; mean diameters of BA-SLN could be maintained only in the presence of threalose and MA-SLN, which were no more dispersible after freeze-drying (Abdelwahed et al. 2005).

Supercooled melts are not unusual in solid lipid nanoparticles systems (Bunjes et al. 1998), the term describes a phenomenon wherein lipid crystallization may not occur although the sample is stored at a temperature below the melting point of the lipid. As the advantage for SLN drug-carrier systems is essentially based on the solid state of the particles, solidification of the particles after coacervation must be verified. The status of lipid particles was investigated using differential scanning calorimetry (DSC).

DSC thermograms of SLN (Figure 2) revealed sharp melting peaks and no supercooled melt was revealed. The experimental melting points and enthalpies for raw lipids and SLN are shown in Table 3. It should be noted that, except for SA, there is only a small difference between melting point of pure lipid and of corresponding SLN. According to Siekmann and Westesen (1994), the melting point decrease of SLN colloidal systems can be due to the colloidal dimensions of the particles, in particular to their high surface-to-volume ratio, and not to recrystallization of the lipid matrices in a metastable polymorph. If the bulk matrix material is turned into SLN, the melting point is depressed (Hunter 1986), the presence of impurities, surfactants and stabilizers could also affect this phenomenon (Hou et al. 2003, Liu et al. 2007).

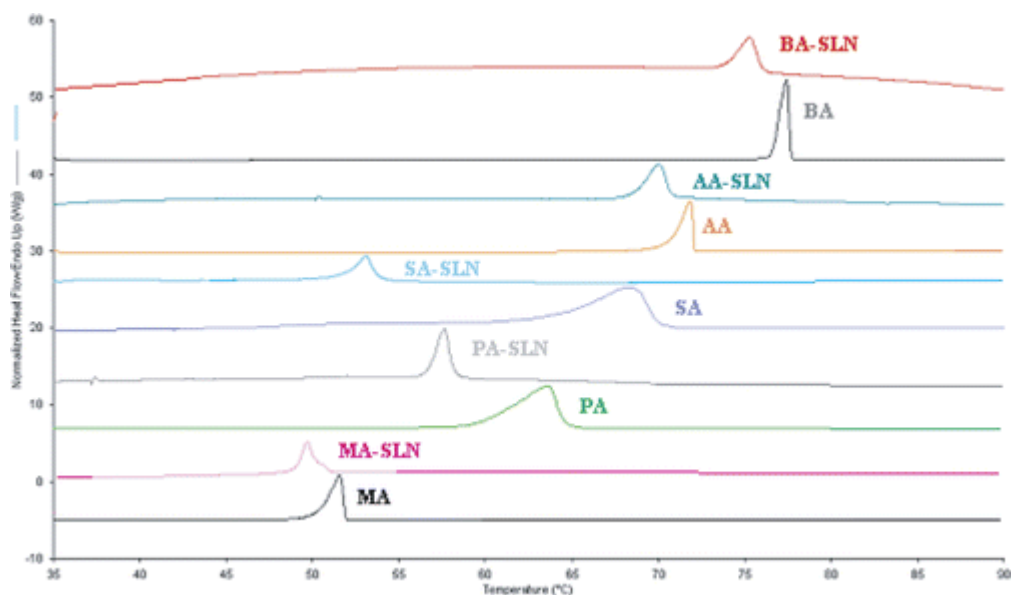


Figure 2. Thermograms of FA-SLN and bulk FA. MA: bulk myristic acid; PA: bulk palmitic acid; SA: bulk stearic acid; BA: bulk behenic acid; AA: bulk arachidic acid; MA-SLN: 1% myristic acid SLN suspension; PA-SLN: 1% palmitic acid SLN suspension; SA-SLN: 1% stearic acid SLN suspension; BA-SLN: 1% behenic acid SLN suspension; AA-SLN: 1% arachidic acid SLN suspension.

Lipid	FA T_{peak} (°C)	FA ΔH (J g ⁻¹)	SLN T_{peak} (°C)	SLN ΔH (J g ⁻¹)	Crystallinity degree (%)
MA	54.6	177.0	49.6	126.7	71.6%
PA	63.6	202.6	57.6	147.1	72.6%
SA	69.8*	211.3*	52.5	46.7	31.1%
AA	75.8	233.9	70.0	208.5	89.1%
BA	79.9	227.1	75.3	179.0	78.8%

SA (B-form): $T_{peak} = 54.5^\circ\text{C}$ and $\Delta H = 150.0 \text{ J g}^{-1}$.

Table 3. FA and FA-SLN melting points (T_{peak}) and melting enthalpies (ΔH).

SA-SLN, instead, have a melting point near to 52°C , quite lower than raw SA (69°C) and this is ascribed to polymorphism. In fact SA can exist in three crystalline forms, A-B-C (Sato 1989), with three different melting points (43°C , 54°C , 69°C , respectively). Further investigation on SA-SLN with X-rays (Figure 3) confirmed that, in SLN, SA was in the low melting B form, which is characterized by monoclinic lattice (Goto and Asada 1978).

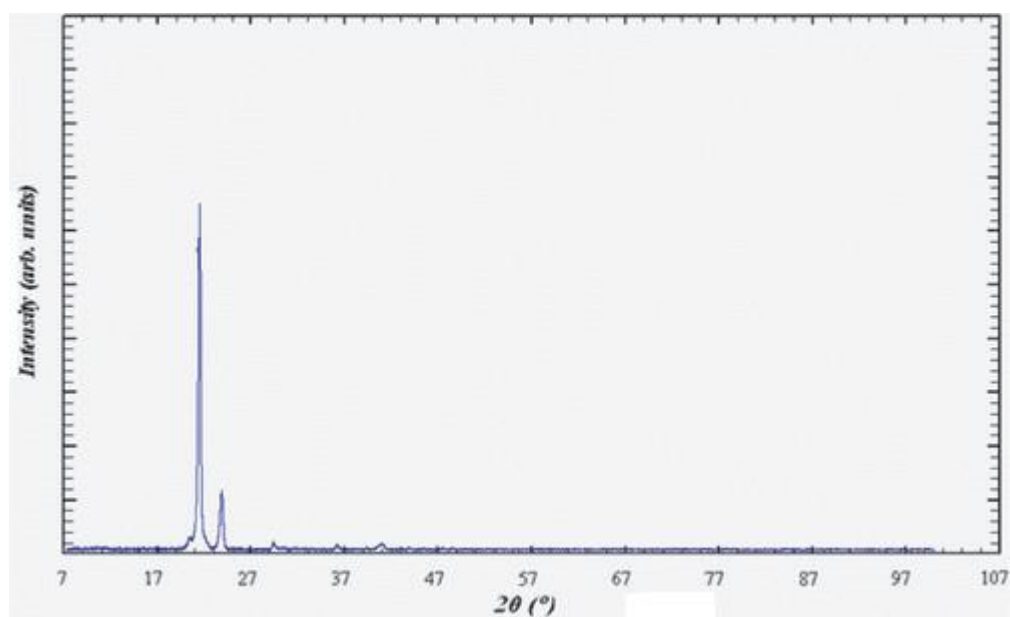


Figure 3. X-rays pattern of SA-SLN.

Successively it was pointed out that SA polymorphism is typical of coacervation process regardless of the presence of a stabilizer. B form of SA was also obtained after acidification of Na-S solution with lactic acid in the absence of PVA. B-form showed a distinct DSC pattern compared to C-form (Figure 4) and proved to be stable upon re-crystallization.

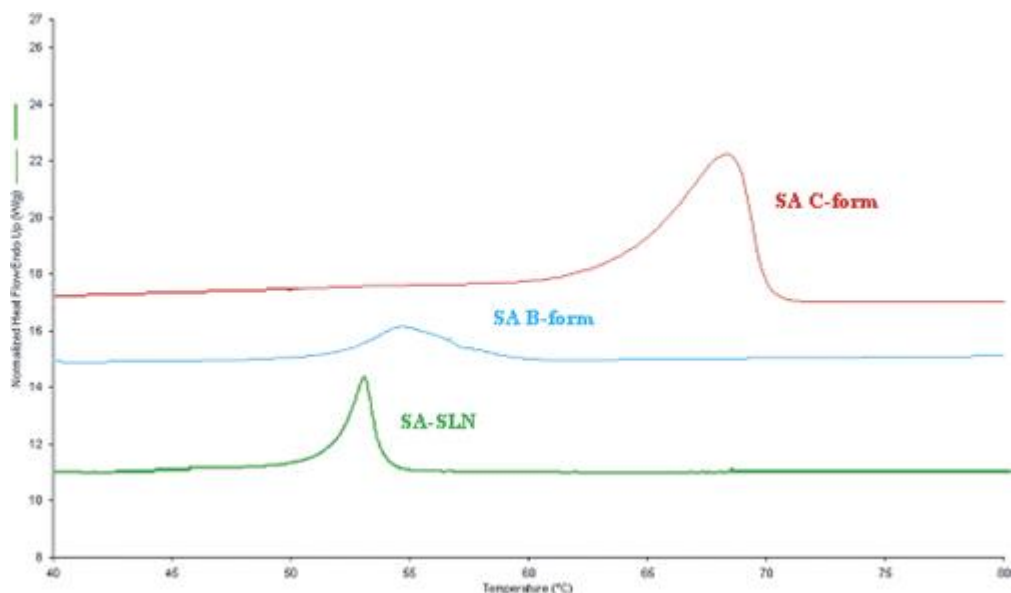


Figure 4. Thermograms of SA in its B and C crystalline forms and of 1%SA-SLN suspension. SA B form: B-polymorph of stearic acid; SA C form: C-polymorph of stearic acid; SA-SLN: 1% stearic acid SLN suspension.

Polymorphism is also documented for PA (α -form melting point 40°C) and MA (α -melting point 24.5°C) (Dupre la Tour 1932, Arutyunova 1963), but in the present experimental conditions SLN don't exhibit polymorph transitions.

Polymorphism has to be taken into account (Müller et al. 2000) for SLN in drug delivery. It is reported for triglycerides that shifts from low melting α or β' form to more stable and high melting β form cause drug release from nanoparticles, because of alteration in lipid matrix crystallinity: so, in the case of polymorphism, the determination of the stability of the crystalline form is very important. In the case of SA-SLN, B-form stability of over 1 month upon storage at room temperature and after freeze-drying was confirmed through DSC measurements.

A degree of crystallinity higher than 70% is obtained for FA-SLN, except for SA-SLN, as shown in Table 3. In the case of SA-SLN, the degree of crystallinity was calculated using the enthalpy of bulk SA in B form, measured on lipid obtained through acidification of Na-S solution with lactic acid.

PA and SA were chosen as lipid matrices for a further formulation study in which different commercially available grades of PVA were used, at the same concentration of PVA 9000. PVA 14 000 and PVA 85 000 caused an increase in particle size and polydispersity compared to PVA 9000: aggregated particles of PA-SLN were obtained in the presence of PVA 14 000 (Table 4).

Polymeric stabilizer	Viscosity ^a (mPa s)	SA-SLN			PA-SLN		
		Mean size (nm)	Polydispersity	ΔH (J g ⁻¹ lipid)	Mean size (nm)	Polydispersity	ΔH (J g ⁻¹ lipid)
PVA 9000 (H.D. 80%)	1.1	285 ± 11	0.015	46.7	263 ± 12	0.018	147.1
PVA 14 000 (H.D. 98%)	1.3	4.82 ± 35	0.131	138.9	ND	ND	192.1
PVA 85 000 (H.D. 89%)	1.9	338 ± 15	0.048	91.3	476 ± 55	0.179	185.1
HPMC 15cP ^c	1.5	394 ± 17 (433 ± 34) ^b	0.060	117.4	/	/	/
HPMC 50cP ^c	2.0	4.97 ± 28 (526 ± 69) ^b	0.114	124.9	/	/	/
HPMC 4000cP ^c	9.8	1448 ± 80 (1617 ± 110) ^b	0.223	103.1	/	/	/

H.D. = hydrolysis degree.

^a determined in 1% w/w aqueous solutions at 48.0 ± 0.5°C in the presence of 1% w/w Na-S.

^b values in brackets are mean sizes after freeze-drying.

^c Substitution degree: 28–30% (methyl); 7–12% (isopropyl).

Table 4. Mean sizes, polydispersities and melting enthalpies (ΔH) of SA-SLN obtained with different PVA and different HPMC 2910 and PA-SLN obtained with different PVA.

PVA type seems therefore to influence nanoparticles mean diameters and polydispersity, probably due to different interactions between lipid and stabilizer, that might depend both on hydrolysis degree and polymer molecular weight.

In the literature it is reported (Hong et al. 2006) that in PVA-stabilized emulsions, low hydrolysis degree of the polymer determines a reduction of emulsion droplet sizes; moreover, it is also well known that an increase of aqueous medium viscosity may cause an increase of SLN particle size (Schubert and Müller-Goymann 2003).

In the present experimental conditions (50°C, in the presence of 1.07% w/w Na-S) only a very slight increase of the viscosity of 1% w/w PVA aqueous solutions was noted as a function of increasing polymer molecular weight. Therefore, viscosity seems not to affect SLN sizes, which might be influenced by polymer hydrolysis degree, probably related to a different interaction of the polymer with nanoparticles surface. As can be noted in Table 4, SLN mean diameters increased as a function of increasing PVA hydrolysis degree: highest values were obtained with PVA 14 000 (hydrolysis degree 98%), followed by PVA 85 000 (hydrolysis degree 89%) and by PVA 9000 (hydrolysis degree 80%).

In Figure 5 DSC patterns of SA-SLN and PA-SLN with different PVA are reported. It can be noted that SA polymorphism is typical of the coacervation process, regardless of the type of PVA used, since the melting point is always near to 52°C (B form). Moreover, transition enthalpies were different according to the stabilizer used, as shown in Table 4: increasing ΔH was recovered following this order: PVA 9000 << PVA 85 000 << PVA 14 000. Therefore, from these data it was supposed that different interactions occurred between the lipid matrix and the polymer used in SLN production.

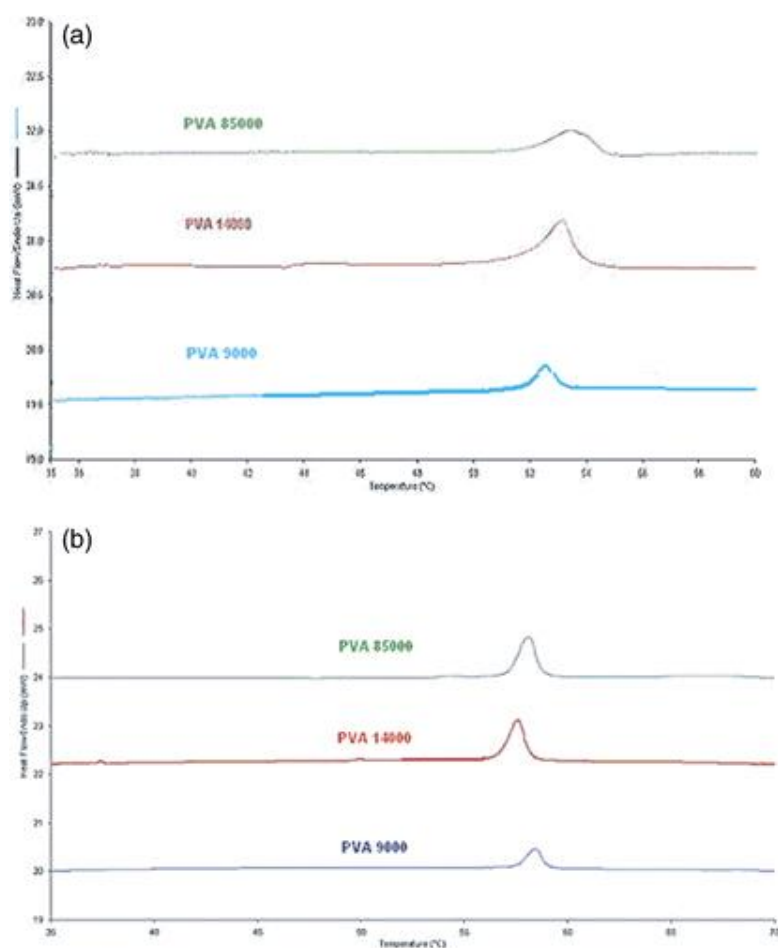


Figure 5. Thermograms of SA-SLN (a) and PA-SLN (b) stabilized with different PVA. (a) 1% SA-SLN suspensions stabilized with: PVA 9000, PVA 14 000, PVA 85 000; (b) 1% PA-SLN suspensions stabilized with: PVA 9000, PVA 14 000, PVA 85 000.

To verify the influence of lipid concentration on SLN characteristics, SA-SLN were prepared at increasing (2%, 5%) lipid concentration in the presence of corresponding amounts of PVA 9000. As can be noted from Table 5, an increasing trend of SLN mean diameters, polydispersities and melting enthalpies was observed on increasing the lipid concentration. It has been previously noticed that PVA 9000-stabilized SLN have a lower melting enthalpy compared to bulk material. The reduction of the melting enthalpy should be due to an interaction between the lipid and the polymer at the surface of nanoparticles. The surface interaction between PVA and SA was supposed to decrease with increasing particle size owing to the consequent reduction of the surface area: such interactions can probably justify the obtained trend of transition enthalpies.

	Mean size (nm)	Polydispersity	ΔH (J g ⁻¹ lipid)
1% SLN	285 ± 11	0.015	46.7
2% SLN	373 ± 18	0.079	87.8
5% SLN	419 ± 50	0.222	139.1

Table 5. Mean sizes, polydispersity and melting enthalpies (ΔH) of 1%, 2%, 5% SA SLN obtained with PVA 9000.

In order to test stabilizers alternative to PVA, different HPMC 2910 (identified by the manufacturer as 25cP, 50cP, 4000cP) having increasing molecular weights, but identical substitution degree, were used at 1% w/w concentration to prepare 1% w/w SA-SLN: also in this case SA was in B form. Particle size, ranging from 400–2000 nm, increased by increasing HPMC molecular weight (Table 4): with HPMC 4000cP microparticles with broad size distribution were obtained. SA-SLN, freeze dried in the absence of cryoprotectant, almost maintain their original mean diameters after suspension in water (Table 4). As the molecular weight of HPMC increased, an increase in viscosity of 1% w/w polymer solution in the presence of 1.07% w/w Na-S was observed at $50 \pm 0.1^\circ\text{C}$ (Table 4). It can therefore be hypothesized that HPMC molecular weight influences SLN particle size, affecting the viscosity of the aqueous medium during coacervation process, as reported in the literature (Schultz and Daniels 2000, Wollenweber et al. 2000). These authors observed an increase of droplet size in O/W emulsions occurring for higher molecular weight HPMC, due to a reduction of HPMC availability at the oil–water interface, because of the stronger polymer intra-chain interactions (expressed as higher viscosities). A similar mechanism might be supposed in SLN stabilization.

Melting enthalpies were found to vary slightly for SLN stabilized with various molecular weight HPMC).

The possibility of application of SLN obtained by the coacervation process in drug delivery was then evaluated using Nile Red, a fluorescent dye, as a lipophilic model substance to be encapsulated in 1% w/w SA-SLN (PVA 9000). SLN of ~ 350 nm (Figure 6) were obtained with an encapsulation efficiency of $92 \pm 0.5\%$.

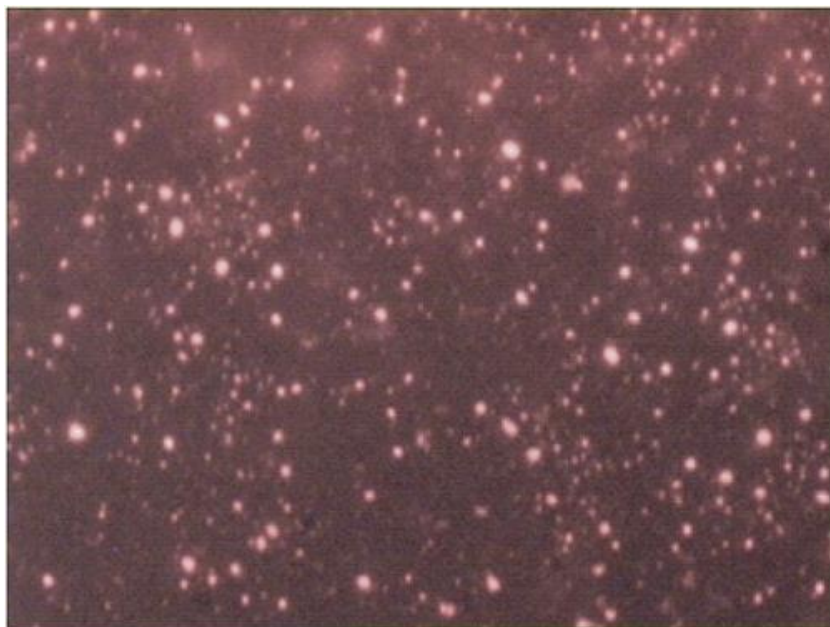


Figure 6. Fluorescence microscope photograph of 1% SA-SLN containing Nile Red.

Conclusions

In this work an innovative process, based on acidic coacervation of fatty acids from their sodium salt micelles in the presence of a stabilizer, is proposed for the SLN production. Close to monodisperse nanoparticles suspensions, easy to be freeze-dried, can be produced. This process presents several advantages, concerning the possibility to overcome many of the formulation problems connected with known techniques. No solvent is used, no sophisticated apparatus is needed, making the method feasible, suitable for laboratory production and easy to scale-up. The coacervation of FA seems to be a promising technique to load lipophilic substances within SLN with good encapsulation efficiency. Further studies are in progress to prepare SLN for drug delivery.

Acknowledgement

This work was supported by a grant from the Italian government (MIUR, Cofin 2006). Declaration of interest: The authors report no conflicts of interest. The authors alone are responsible for the content and writing of the paper

References

1. Abdelwahed W, Degobert G, Fessi H. A pilot study of freeze drying of poly(epsilon-caprolactone) nanocapsules stabilised by poly(vinyl alcohol): Formulation and process optimisation. *Int J Pharm* 2005; 309: 178–188
2. Arutyunova LB. Simultaneous microthermal and spectroscopic study of higher fatty acids. *Zhurnal Fizicheskoi Khimii* 1963; 37: 2413–2419
3. Battaglia L, Trotta M, Gallarate M, Carlotti ME, Zara GP, Bargoni A. Solvent lipid nanoparticles formed by solvent-in-water emulsion diffusion technique: Development and influence of insulin stability. *J Microencapsulation* 2007; 14: 672–684
4. Bunjes H, Siekmann B, Westesen K. Emulsion of supercooled melts, a novel drug delivery system. Submicron emulsions in drug targeting and delivery, S Benita. Harwood Academic Publisher, Amsterdam 1998; 175–205
5. Dupre la Tour F. X-ray study of the polymorphism of the normal saturated acids of the aliphatic series. *Ann Phys* 1932; 18: 199–283
6. Freitas C, Müller RH. Correlation between long-term stability of solid lipid nanoparticles (SLN™) and crystallinity of the lipid phase. *Eur J Pharm Biopharm* 1999; 47: 125–132
7. Gallarate M, Trotta M, Battaglia L, Chirio D. Preparation of solid lipid nanoparticles from W/O/W emulsions: Preliminary studies on insulin encapsulation. *J Microencapsulation* 2008; 3: 1–9
8. Gasco MR. US Patent n° 5250236. 1993
9. Goto M, Asada E. The crystal structure of the B-form of stearic acid. *Bull Chem Soc Jap* 1978; 51: 2456–2459
10. Hong S, Albu R, Labbe C, Lasuye T, Stasik B, Riess G. Preparation and characterisation of colloidal dispersions of vinyl alcohol-vinyl acetate copolymers: Application as stabilisers for vinyl chloride suspension polymerisation. *Polym Int* 2006; 55: 1426–1434
11. Hou D, Xie C, Huang K, Zhu C. The production and characteristics of solid lipid nanoparticles (SLN). *Biomaterials* 2003; 24: 1781–1785
12. Hunter RJ. Foundation of colloidal science. Oxford University Press, Oxford 1986
13. Lin B, McCormick AV, Davis HT, Strey R. Solubility of sodium soaps in aqueous salt solutions. *J Coll Surface Sci* 2005; 291: 543–549
14. Liu J, Gong T, Wang C, Zhong Z, Zhang Z. Solid lipid nanoparticles loaded with insulin by sodium cholate-phosphatidylcholine-based mixed micelles. Preparation and characterisation. *Int J Pharm* 2007; 340: 153–162

15. Müller RH, Lucks JS. Eur patent n° 06055497. 1996
16. Müller RH, Mäder K, Gohla S. Solid lipid nanoparticles (SLN) for controlled drug delivery—a review of the state of the art. *Eur J Pharm Biopharm* 2000; 50: 161–177
17. Maculotti K, Enrica Tira M, Sonaggere M, Perugini P, Conti B, Modena T, et al. In vitro evaluation of chondroitin sulfate-chitosan microspheres as carrier for the delivery of proteins. *J Microencapsulation* 2008; 9: 1–9
18. Mumper RJ, Jay M. US patent n° 7153525. 2006
19. Sato K. Solvent effects on crystallization of polymorphic modifications of lipids, morphology and growth unit of crystals. Terrapub, Tokyo 1989; 513
20. Scholes PD, Coombes AGA, Illum L, Davis SS, Watts JF, Ustariz C, et al. Detection and determination of surface levels of poloxamer and PVA surfactant on biodegradable nanospheres using SSIMS and XPS. *J Contr Rel* 1999; 59: 261–278
21. Schubert MA, Müller-Goymann CC. Solvent injection as a new approach for manufacturing lipid nanoparticles—evaluation of the method and process parameters. *Eur J Pharm Biopharm* 2003; 55: 125–131
22. Schultz M, Daniels R. Hydroxypropylmethylcellulose (HPMC) as emulsifier for submicronemulsions: Influence of molecular weight and substitution type on the droplet size after high-pressure homogenisation. *Eur J Pharm Biopharm* 2000; 49: 231–236
23. Shinoda K. Solvent properties of surfactant solutions. Dekker, New York 1967; 2
24. Siekmann B, Westesen K. Investigation on solid lipid nanoparticles prepared by precipitation in o/w emulsion. *Eur J Pharm Biopharm* 1996; 43: 104–109
25. Siekmann B, Westesen K. Thermoanalysis of the recrystallization process of melt-homogenized glyceride nanoparticles. *Colloid Surf B* 1994; 3: 159–175
26. Silva MA, Franco DF, De Oliveira LF. New insight on the structural trends of polyphosphate coacervation processes. *J Phys Chem A* 2008; 112: 5385–5389
27. Trotta M, Cavalli R, Carlotti ME, Battaglia L, Debernardi F. Solid lipid micro-particles carrying insulin formed by solvent-in-water emulsion-diffusion technique. *Int J Pharm* 2005; 288: 281–288
28. Wen X, Franses EI. Effect of protonation on the solution and phase behavior of aqueous sodium myristate. *J Coll Surf Sci* 2000; 231: 42–51
29. Wollenweber C, Makievski AV, Miller R, Daniels R. Adsorption of hydroxypropyl methylcellulose at the liquid:liquid interface and the effect on emulsion stability. *Colloids Surf A Physicochem Eng Aspects* 2000; 172: 91–101